Role of the Biomimetic Scaffolds in the Regeneration of Articular Tissue in Deep Osteochondral Defects in a Rabbit Model

PAL FODOR[1], ARPAD SOLYON[2]*, RALUCA FODOR[2], CORNEL CATOI[3], FLAVIU TABARAN[3], RADU LACATUS[3], CRISTIAN TRAMBITAS[2], TIBERIU BATAGA[3]

Clinical County Emergency Hospital Mures, 50 Gheorghe Marinescu Str., 540136, Targu Mures, Romania
University of Medicine and Pharmacy of Tirgu Mures, 38 Gheorghe Marinescu Str., 540139, Tirgu Mures, Romania
University of Agricultural Sciences and Veterinary Medicine 3-5 Manastiur Road, 400372, Cluj-Napoca, Romania

The ability of damaged articular cartilage to recover with normal hyaline cartilage is limited. Our aim was to study the mechanism of in vivo cartilage repair in case of severe osteochondral lesions using a three-dimensional matrix implanted without any preseeded cells in the osteochondral defect in a rabbit model. According to the ICRS scores from macroscopic observations of the femoral condyles, the average scores in the scaffold groups were higher than those in the control groups at every time ($P<0.001$). Histological examination of the ostheochondral defects, revealed regeneration of new tissue with hyaline-like cartilage features only in matrix groups. At twelve weeks from implantation, complete filling of the defect with hyaline cartilage with a tendency of mineralization and the absence of implant material is observed. The superficial area of the defect is completely covered with hyaline-like cartilage. The scaffold used leaded to the regeneration of articular tissue with an ordered histoarchitecture.

Key words: osteochondral defect, scaffold, hyaline cartilage, mineralization

Articular cartilage is a glass-like (hyaline), flexible but strong supportive connective tissue that covers joint surfaces [1]. It provides a low-friction and lubricated surface facilitating the transmission of loads to the underlying subchondral bone [2]. It has a simple structure made up of articular cartilage cells and extracellular matrix rich in water along with type II collagen, proteoglycans, and structural glycoproteins. The chondrocytes are isolated cells embedded in lacunae able to exist in a low-oxygen environment [3]. They occupy only about 5% of the tissue volume and are responsible for matrix synthesis and turnover [4].

Articular cartilage is susceptible to both traumatic injury and degenerative disease [5]. The ability of damaged articular cartilage to recover with normal hyaline cartilage is limited because of two main factors: the inability of the undifferentiated cell population to leave their territory through the dense matrix, and the little potential to increase their metabolic rate to regenerate neotissue because of the absence of blood vessels and innervation [4, 5].

The space between the articular cartilage and cancellous bone of the epiphysis is occupied by subchondral bone, which also intervenes in distributing the loads between the articular cartilage and the stiff cancellous and cortical bone. It is composed of dense collagen fibers and intracellular substance saturated with calcium and phosphorus minerals [3, 6]. In case of deep subchondral injuries, when the defect is exposed to the bone marrow, and is not treated properly, it results in the formation of a fibrous cartilage with inferior mechanical properties for the load-bearing environment of the joint [7]. In these cases the osteoarthritis symptoms can be seen radiographically after 10 years and primary gonarthrosis related with osteoarthritis develops 10 years early [5, 8].

Orthopedic surgeons have developed several surgical methods in order to resurface the damaged articular cartilage and/or subchondral bone. These range from purely palliative treatments such as arthroscopic debridement to reparative techniques which aim to stimulate fibrous repair tissue (drilling, microfracture) [4] and finally to regenerative methods which aim to replace the damaged cells and intracellular substance while preserving their microarchitecture and biomechanical function of the tissues [3]. Regenerative methods include: techniques based on osteochondral transplantation (mosaicplasty) [9], cell-based approaches (e.g. autologous chondrocyte implantation) [10] and a more recently tissue engineering techniques using scaffolds. Clinical results with various methods of cartilage repair are not always adequate. Microfractures lead to predominantly fibrous type cartilage tissue at the repair site. Mosaicplasty may be limited by the size of the injured area and involves surgical aggression in both the donor and receptor regions of the osteochondral graft [4]. Autologous chondrocyte implantation adding the autogenous bone implant before the implantation of autologous chondrocytes [11] has been shown to better stimulate the production of hyaline-like repair tissue [10]. It has been successfully applied for more than a decade and is considered the gold standard in the reparation of osteochondral injuries [4]. But, the technique is expensive and involves two surgical procedures, due to the requirement of off-site isolation and culturing of the chondrocyte cell line performed several months apart, which implies long functional recovery times [11].

Our aim was to study the mechanism of in vivo cartilage repair in case of severe osteochondral lesions using tissue engineering technique. The cell source was mesenchymal stem cells migrating from subchondral bone and invading a three-dimensional matrix that was implanted without any preseeded cells in the osteochondral defect, thereby maintaining mechanical integrity.

Experimental part

Materials and methods

Animal care

Our study included 12 six-month-old male rabbits, weighing 1.5 kg to 3.0 kg. The 12 rabbits were randomly divided into 2 experimental groups of 12 knees per group.

* email: solyomarpad@yahoo.com; Phone: (+40)740695460

All experimental procedures with animals followed the international recommendations for the use and care of animals and the study protocols were approved by Institutional Review Board of University of Medicine and Pharmacy Targu Mures no. 35 from 21st of March 2016. The animals were acclimatized to the usual laboratory conditions 7 days before the experiment and were housed with appropriate bedding and provided water ad libitum and free access to standard laboratory rodent feed. Rabbits were kept in standard single cages under controlled temperature and light conditions.

Experimental design

After 4 h of stopping nutrition, each animal was sedated by intramuscular injection of ketamine hydrochloride 60 mg/kg and xylazine 6 mg/kg. This drug combination ensures post procedural analgesia also. In sterile conditions, a medial para-patellar arthrotomy was made in both knees. A full-thickness cylindrical osteochondral defect of 5 mm in diameter and 8 mm in depth was created in the patellar groove through use of a standard size drill head (fig. 1A). In experimental animals, the defect area of right knee was treated by implanting a of a biomimetic ostechondral scaffold (MaioRegen; Fin-Ceramica Faenza SpA, Faenza, Italy) press fit into the area (fig. 1B), whereas the defect area of left knee was left untreated. The stability of the implanted scaffold was tested by cyclic flexion-extension of the knee while the graft was visualized. After the surgery, the knee joint capsule and skin were closed using resorb able surgical sutures. The rabbits were allowed to move freely postoperatively. To avoid the postoperative infections, antibiotic injections were given three days postoperative.

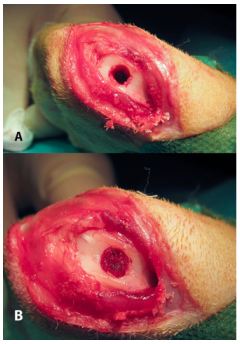

Fig. 1. Experimental model
A- A full-thickness cylindrical osteochondral defect of 5 mm in diameter and 8 mm in depth was created in the patellar groove in both knees of all studied animals; B- The defect area of right knee of all the studied animals was treated by implanting a of a biomimetic osteochondral scaffold (MaioRegen) press fit into the area.

At six and twelve weeks after implantation, the rabbits in each group were sacrificed by injecting pentobarbital sodium (>100 mg/kg intraperitoneal), according to Annex IV from Directive 2010/63/UE – L 276/72. Both knees were excised, photographed and graded for cartilage repair, according to the international cartilage repair society score (ICRS) macroscopic assessment scores (table 1). Afterwards, the joints were CT scanned and further processed for the histological analysis.

Histopathological examination

For the histopathological examination, the femoral condyles were fixed for 7 days by immersion in 10% neutral-buffered formalin (NBF). Following complete aldehyde fixation, the femoral condyles were cleaned of muscle and connective tissue and decalcified for two weeks in a 1:1 mixture of formic and hydrochloric acid (8%). When decalcification was completed, the tissues were transversely trimmed, briefly washed in tap water and dehydrated in ethylic alcohol in ascending concentration (70, 80, 90, 95, and 100%), clarified in xylene and embedded in high temperature melting paraffin wax. Tissue sections were cut from each paraffin block at 4 μm thickness with a rotary microtome and routinely stained with haematoxylin and eosin (H&E). The histological slides were examined using an Olympus BX41. Images and morphometric evaluation were obtained with an Olympus UC30 digital camera.

The re-created tissue was scored blindly according to the ICRS scale (table 2).

Statistical analysis

For statistical analysis we used SPSS version 20 (USA, CA). In order to characterize groups we employed descriptive statistics (mean, standard deviation, minimum, maximum). The means between groups were compared for statistical significance using the t-test for Equality of Means. The confidence intervals were set at a 95%. A value of $p<0.05$ was considered statistically significant.

Results and discussions

Macroscopic observation

All rabbits in the experimental groups, survived the follow-up period of six and twelve weeks without wound infection, or synovitis in the operated knees.

Categories	Score
Degree of defect repair	
In level with surrounding cartilage	4
75% repair of defect depth	3
50% repair of defect depth	2
25% repair of defect depth	1
Integration to border zone	
Complete integration with surrounding cartilage	4
Demarcating border <1 mm	3
3/4 of graft integrated, 1/4 with a notable border >1 mm width	2
1/2 of graft integrated with surrounding cartilage, 1/2 with a notable border >1 mm	1
From no contact to 1/4 of graft integrated with surrounding cartilage	0
Macroscopic appearance	
Intact smooth surface	4
Fibrillated surface	3
Small, scattered fissures or cracks	2
Several, small or few but large fissures	1
Total degeneration of grafted area	0
Overall repair assessment	
Grade I: normal	12
Grade II: nearly normal	11-8
Grade III: abnormal	7-4
Grade IV: severely abnormal	3-1

Table 1
ICRS MACROSCOPIC EVALUATION OF CARTILAGE REPAIR [12]

Table 2
ICRS VISUAL HISTOLOGICAL ASSESSMENT SCALE [13]

Feature	Score
I. Surface	
Smooth/continuous	3
Discontinuities/irregularities	0
II. Matrix	
Hyaline	3
Mixture: Hyaline/fibrocartilage	2
Fibrocartilage	1
Fibrous tissue	0
III. Cell distribution	
Columnar	3
Mixed/columnar-clusters	2
Clusters	1
Individual cells/disorganized	0
IV. Cell population viability	
Predominantly viable	3
Partially viable	1
<10% viable	0
V. Subchondral Bone	
Normal	3
Increased remodeling	2
Bone necrosis/granulation tissue	1
Detached/fracture/callus at base	0
VI. Cartilage mineralization (calcified cartilage)	
Normal	3
Abnormal/inappropriate location	0

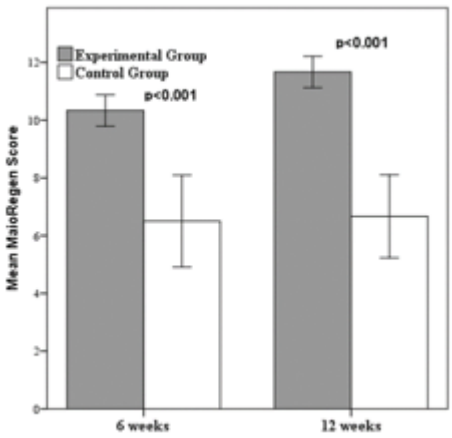

Fig. 3. ICRS macroscopic evaluation of cartilage repair. The statistical differences between the Maioregen groups and control groups were significant at six weeks and again at 12 weeks (P<0.001).

The macroscopic evaluation of the femoral condyles in MaioRegen group at sixt weeks, revealed regenerated tissue although the boundary was still notable between the defective tissue and the normal tissue. At twelve weeks, in MaioRegen group the implant was found to be completely covered with cartilage-like, whitish, glossy tissue which was well integrated into the surrounding cartilage as compared with control group (fig. 2). According to the ICRS scores from macroscopic observations of the femoral condyles, the average scores in the MaioRegen groups were higher than those in the control groups at every time (fig. 3).

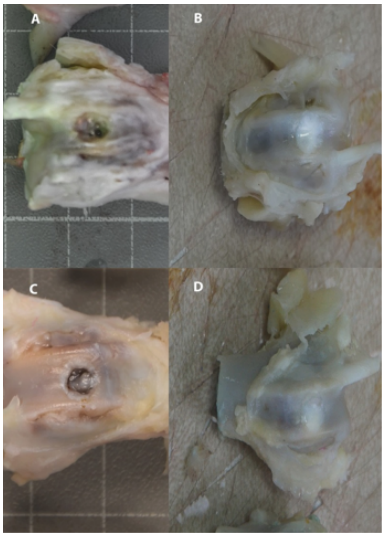

Fig. 2. Gross appearance of defects in the trochlear groove. A) Control group at six weeks – no implant. The defect is partially vacant and clearly noticeable from the surrounding cartilage. B) Maioregen group at six weeks. Repaired tissue covers the defect completely, but is distinguishable from the surrounding cartilage. C) Control group at twelve weeks – no implant. The defect is still partially vacant and clearly noticeable from the surrounding cartilage. D) Maioregen group at twelve weeks. Repaired tissue covers the defect completely and no obvious margin was notable

Joints CT scanned

Joints CT scanned evaluation showed the appearance of newly formed bone in the deepest area of the defect in the MaioRegen groups (fig. 4B, 4D). The subchondral bone healing was observed in experimental groups in a time dependent manner, when compared to the control group, which showed only lytic holes.

Histological examination

Histological assessment confirmed the macroscopic results. The mean results of the histological assessment are presented in figure 5-10. The values in MaioRegen

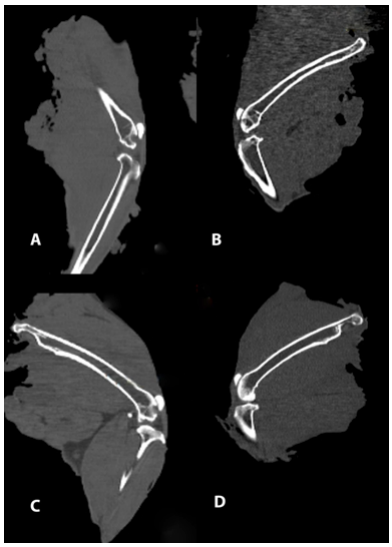

Fig. 4. Joints CT scanned images
A) Control group at six weeks – no implant. Lytic hole, no newly formed bone in the defect area. B) Maioregen group at six weeks. The defect is partially filled with newly formed bone. C) Control group at twelve weeks – no implant. Minimal bone formation in the defect area, with the presence of multiple cysts. D) Maioregen group at twelve weeks. Complete filling of the defect with newly formed bone.

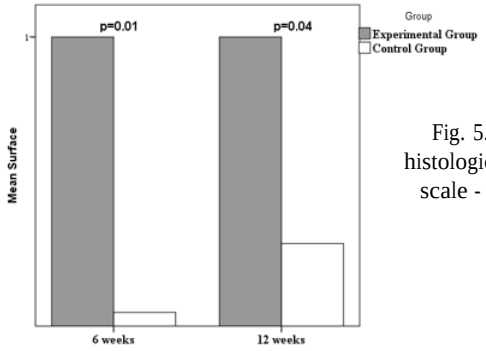

Fig. 5. ICRS visual histological assessment scale - Mean Surface

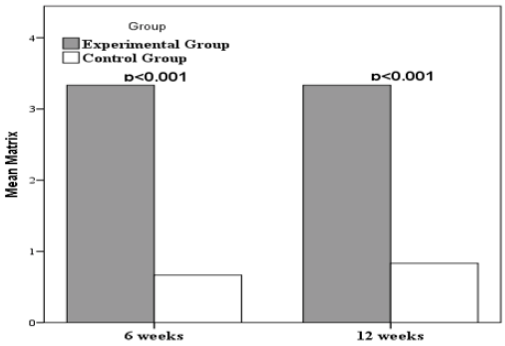

Fig. 6. ICRS visual histological assessment scale - Mean Matrix

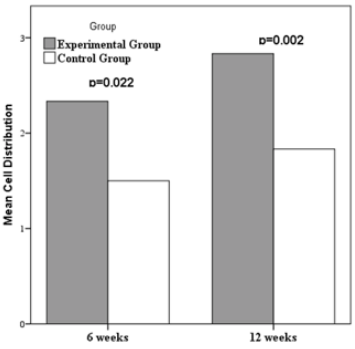

Fig. 7. ICRS visual histological assessment scale - Mean Cell Distribution

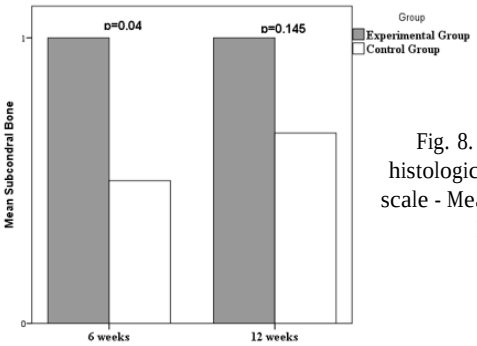

Fig. 8. ICRS visual histological assessment scale - Mean Subchondral Bone

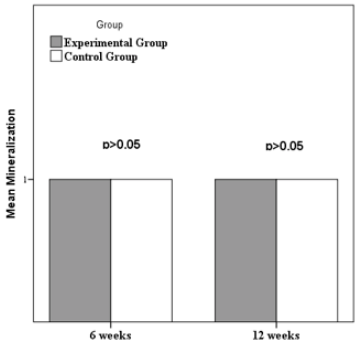

Fig. 9. ICRS visual histological assessment scale - Mean Mineralization

groups after six and 12 weeks of observation were statistically significant higher compared to control groups in all criteria, except mean mineralization. Histological examination of the ostheochondral defects, revealed regeneration of new tissue with hyaline-like cartilage features only in MaioRegen groups (fig. 11, 13). Histological features of biopsy specimens taken at 6 weeks from

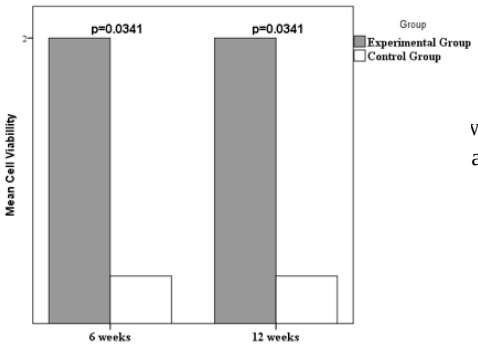

Fig. 10. ICRS visual histological assessment scale - Mean Cell Viability

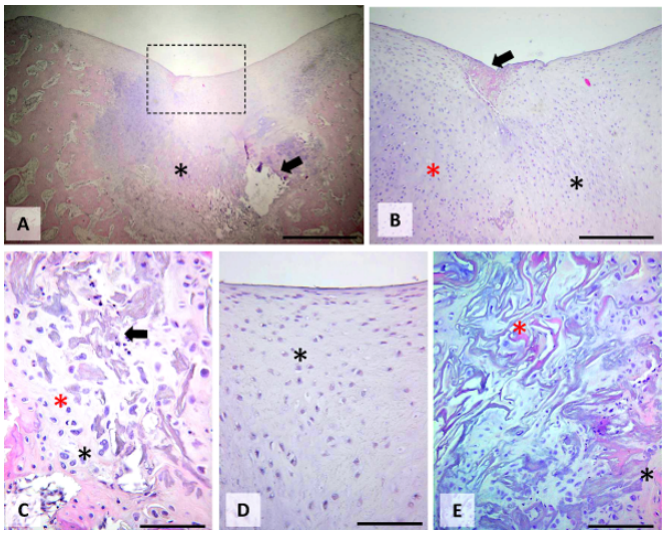

Fig. 11. The histopathological examination of the femoral trochlea from the MaioRegen group at 6 weeks.
Picture A captures the cross-sectional appearance of the femoral trochlea and the induced defect (marked by black asterisk). We observe the total coverage of the defect with cartilaginous tissue in admixture with the scaffold (reticular, basophilic aspect). The arrow indicates the presence of a cavitary aspect between the cartilage tissue mass and the underlying bone.Picture B represents the histological detail of the area marked by a rectangle in the image A. Compete filling of the defect with cartilage tissue (hyaline cartilage-red asterisk, respectively fibrocartilage-black asterisk) is observed. Focal persistence of superficial necrotic material (arrow).Picture C represents the deep defect area characterized by the presence of cartilaginous tissue (black asterisk) with areas of bone metaplasia (red asterisk) and implant material (reticular, basophilic possibly mineralized) (arrow).Picture D shows the superficial appearance of hyaline cartilage with the specific chondrocyte distribution.Picture E shows the deep defect area where the focal presence of the implant material is observed (with onset of mineralization), lax fibrous connective tissue (red asterisk) and cartilaginous tissue with bone metaplasia (black asterisk).H & E, ob x 4 for image A (scale = 1000 μm), obx20 for image B (scale = 200 μm), obx40 for C, D and E images (scale = 100 μm).

implantation demonstrated the coverage of the defect with cartilaginous tissue in admixture with the scaffold and areas of bone metaplasia (fig. 11) suggesting that the repair tissue was still undergoing remodeling. It was also observed a superficial appearance of hyaline cartilage with the specific chondrocyte distribution (fig. 11D). By contrast in the control group at six weeks, the neotissue fills incompletely the ostheochondral defect and is characterized by the presence of fibrotic scar tissue in various stages of maturity (fig. 12).

At twelve weeks from implantation, complete filling of the defect with hyaline cartilage with a tendency of mineralization and the absence of implant material is

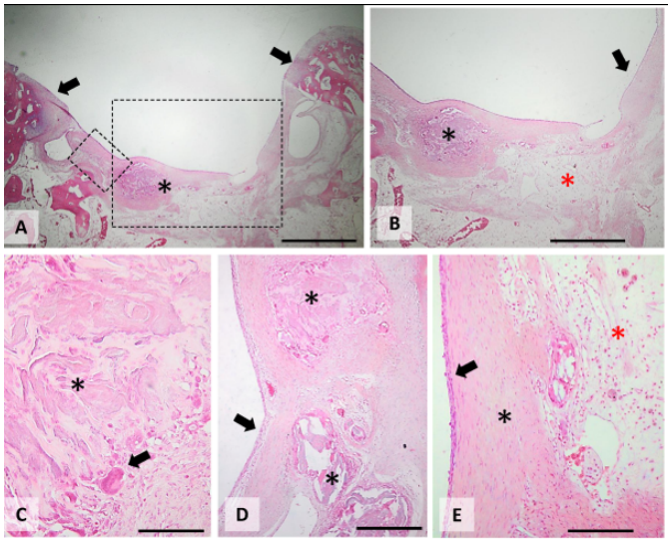

Fig. 12. Histopathological examination of the femoral trochlea from the control group at 6 weeks.
Picture A captures the cross-sectional appearance of the femoral trochlea and the induced defect (marked by black asterisk). Arrows indicate the marginal area of the defect. The neotissue fills incompletely the ostheochondral defect and is characterized by the presence of fibrotic scar tissue in various stages of maturity (the dominant structure) and a discreet marginal cartilaginous tissue (minimal, in shape of a border). Noteworthy the presence of inflammatory outbreaks characterized by the presence of bone detritus and the marginal resorption border (marked by asterisk). Picture B represents the histological detail of the area demarcated by a rectangle on the right side of image A. The defect is incompletely filled with fibrous scar tissue in the deep area (red asterisk) with a superficial layer of mature tissue. Noteworthy the inflammatory outbreaks characterized by the presence of bone detritus and a marginal resorption border (black asterisk). Picture C represents the histological detail of the deep defect area. The presence of bone detritus is observed (acidophilic, amorphous, indicated by asterisk) with marginal inflammatory resorption border (granulomatous foreign body reaction) (indicated by arrow). Picture D represents the histological detail of the area demarcated by the rectangle on the left side of image A. It shows the superficial appearance of the defect, characterized by scar conjunctival tissue with outbreaks containing bone detritus (asterisk) and secondary inflammation. Picture E represents the histological detail of the superficial area of the defect. The defect is filled with fibrous lax scar tissue in the deep area (red asterisk), and a superficial layer of mature tissue (black asterisk). H & E, ob x 4 for image A (scale = 1000 μm), obx10 for image B (scale = 400 μm), obx40 for C, D and E images (scale = 100μm)

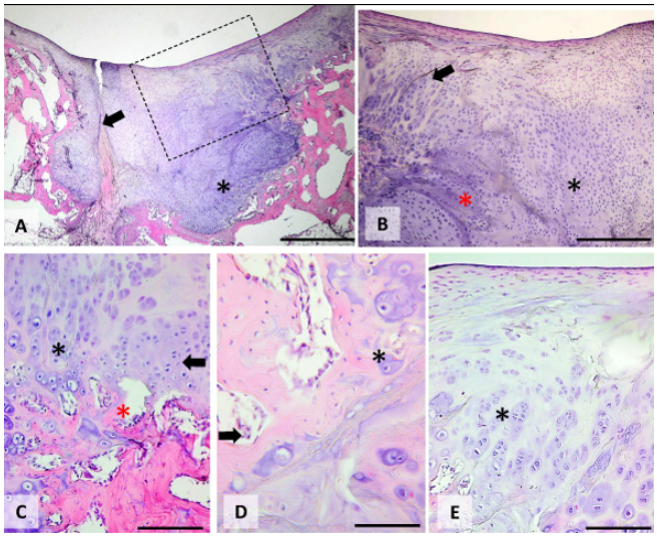

Fig. 13. Histopathological examination of the femoral trochlea from the MaioRegen group at 12 weeks;
Picture A captures the cross-sectional appearance of the femoral trochlea and the induced defect (marked by black asterisk). The total defect coverage with cartilaginous tissue is noticed. The arrow indicates the presence of a complete vertical defect in the cartilage tissue mass. Picture B represents the histological detail of the area demarcated by a rectangle in image A. Complete filling of the defect with cartilage tissue is observed (hyaline cartilage - black asterisk and hyaline cartilage with a tendency of mineralization - onset of bone metaplasia - red asterisk). The arrow shows the tendency of the chondrocytes to order in cords (corresponding to the area of proliferation in endochondral ossification). Picture C represents the deep area of the defect characterized by the presence of cartilaginous tissue (black asterisk) with bone metaplasia areas (red asterisk). The arrow shows the tendency of the chondrocytes to order in cords (corresponding to the area of proliferation in endochondral ossification); Note the absence of implant material. Picture D represents the deep area of the defect characterized by endochondral ossification (black asterisk) and osteoblast activation (arrow); Picture E represents the superficial area of the defect with the presence of hyaline-like cartilage with onset of bone metaplasia (asterisk). H & E, ob x 4 for image A (scale = 1000 μm), obx20 for image B (scale = 200μm), obx40 for C, D and E images (scale = 100 μm)

observed (fig. 13). The superficial area of the defect is completely covered with hyaline-like cartilage. In the control group at twelve weeks, the defect area is filled with cartilaginous tissue (fibrocartilage) with only a marginal bone metaplasia and not integrated with the host cartilage (fig. 14).

More than 2.2 million bone graft procedures are performed annually worldwide to fill defects [14]. Over the last decade, a number of natural and artificial biomaterials have been used as scaffolds for cartilage reformation. Scaffolds may be monophasic, biphasic, triphasic or multiphasic in structure, consisting of one or more layers [10]. They play important roles in maintaining mechanical integrity and withstanding mechanical stresses [4]. To date, no tissue engineered osteochondral construct has yet regenerated functional tissues that possess the properties of native cartilage and bone, but have the potential to delay further degenerative changes and may eliminate the need for total joint replacements in the long term [10].

Artificial materials were used in biomedicine because of their superior mechanical properties, and biodegradability, but their poor biocompatibility has limited their application [15]. Natural materials, such as collagen [16, 17], chitosan [18-20], alginate [21, 22] and hyaluronic acid [23-25] have been studied and obtained promising results [1].

Varying cell types and growth factors may be introduced into each layer to encourage the regeneration of cartilage and bone tissue. But, scaffolds capable of in vivo regeneration utilizing the body's own endogenous cells were also described [10].

Currently, only a few scaffolds have obtained the European Conformity (CE) certification and are available for clinical application in Europe [11].

We used for this study the MaioRegen scaffold, which is a three-dimensional matrix which mimics the entire osteo-cartilaginous tissue: cartilage, tide mark and sub-chondral bone. It is a monolithic, multi-layer scaffold, and its composition is based on nucleation of hydroxyapatite

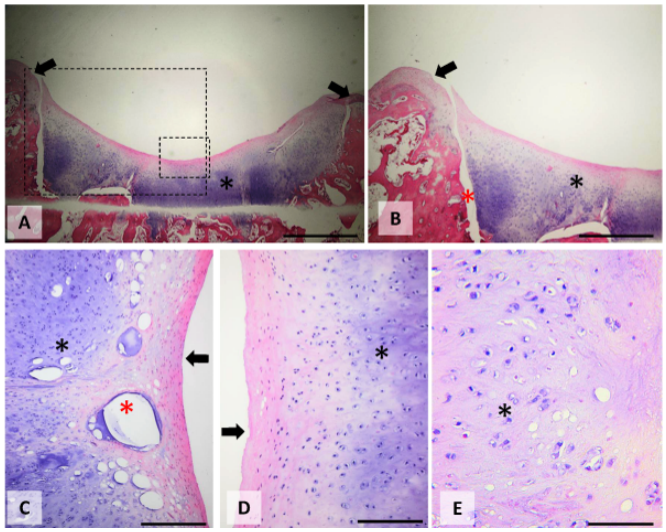

Fig. 14. Histopathological examination of the femoral trochlea from the control group at 12 weeks.
Picture A captures the cross-sectional appearance of the femoral trochlea and the induced defect (marked by black asterisk). Arrows indicate the marginal area of the defect not integrated with the host cartilage. The defect area is filled with cartilaginous tissue. (Fibrocartilage). Picture B represents the histological detail of the area demarcated by the rectangle on the left side of image A. It is noticeable that the defect is filled with cartilaginous tissue (black asterisk) with marginal bone metaplasia (characterized by basophilia secondary to mineralization). The red asterisk marks the cleavage area between the regenerated cartilage and the marginal bone.(host tissue) Picture C and D represent the histological detail of the superficial area of the defect, (image D - the area demarcated by the rectangle in the center of the image A). The defect is filled with cartilaginous tissue (black asterisk) with a superficial layer of fibrocartilaginous tissue (arrow). The red asterisk indicates areas of cystic, cavitary appearance, present in the superficial area of the cartilage. Picture E represents the deep area of the defect characterized by the presence of fibrous cartilage tissue. H & E, ob x 4 for image A (scale = 1000 µm), obx20 for image B (scale = 200 µm), obx40 for C and D, and obx20 for images E (scale = 40 µm).

nanocrystals onto self-assembled collagen fibers. Magnesium ions have been introduced to increase the physicochemical, structural, and morphological affinities of the composite with natural bone [26]. The superficial layer consists of deantigenated type 1 equine collagen and resembles the cartilaginous tissue, while the lower layer consists mostly of magnesium enriched Hydroxyapatite (Mg-HA) (70%) and simulates the sub-chondral bone structure. The middle layer, composed of Mg-HA (40%) and collagen (60%), reproduces the tide mark [27]. This scaffold was developed to promote the processes of tissue regeneration in case of large chondral (grade III and IV according to Outerbridge classifcation) and osteochondral lesions [28].

It is an acellular biomaterial that offered few advantageous properties such as lack of donor-site morbidity, absence of cell culture costs, off the shelf availability and application of one-stage surgical procedures [29]. Experimental studies showed that, similar results were obtained with or without loading the implant with cultured autologous chondrocytes [30, 31].

Similar to other studies [32-34], in the present animal model the scaffold rapidly filled the osteochondral defects and induced an ordered in situ regeneration, possibly through mesenchymal stem cells migrating from the bone marrow surrounding the implantation site. This allowed the regeneration of a good quality and well-integrated tissue. Histological evaluation showed complete filling of the defect with hyaline cartilage with a tendency of mineralization and the absence of implant material only in Maioregen groups. Although, the maturation of the deep neotissue was still underway, the regeneration of articular cartilage we observed agrees with previous studies where hyaline cartilage was described on the top of the defect, using different biomaterials [35].

In good agreement with the literature, the twelve weeks follow-up results in the control group indicated poor spontaneous healing of the osteochondral defect in this rabbit model. We found predominantly fibrous type cartilage tissue at the repair site with limited filling of the defect and poor integration with the surrounding tissue.

Also, the mean results of the histological assessment were significant higher in MaioRegen groups compared to control groups. This demonstrates the better quality of the newly formed tissue on the bases of the biomaterial.

Conclusions

We confirmed the better quality of the newly formed tissue on the basis of biomaterial in case of deep ostheochondral defect. The scaffold used leaded to the regeneration of articular tissue with an ordered histoarchitecture. Superficial articular cartilage regenerated 3 months after implantation, with the appearance of hyaline-like cartilage covering.

References

1.POT, M., GONZALES, V., BUMA, P., INTHOUT, J., VAN KUPPEVELT, T H., DAAMEN, W. PeerJ., **4**:e2243; DOI 10.7717/peerj.2243.
2.SOPHIA FOX AJ, BEDI A, RODEO SA. Sports Health., **1**, nr 6, 2009, p. 461.
3.ZYLINSKA, B., STODOLAK-ZYCH, E., SOBCZYNSKA-RAK, A., SZPONDER, T., SILMANOWICZ, P., LANCUT, M., JAROSZ, L., RÓZAÑSKI, P., POLKOWSKA, I., In vivo., **31**,2017, p. 895.
4.SANCHO-TELLO, M., FORRIOL, F., GASTALDI, P., RUIZ-SAURI, A., MARTÍN DE LLANO, J., NOVELLA-MAESTRE, E., ANTOLINOS-TURPIN, C., GOMEZ-TEJEDOR, J., GOMEZ RIBELLES, J., CARMEN CARDA, C., Int J Artif Organs., **38**, nr 4, 2015, p. 210.
5.OZMERIÇ, A., ALEMDAROGLU, K. B., AYDOGAN, N. H., World J Orthop., **5**, nr. 5, 2014, p. 677.
6.DING, M., DALSTRA, M., LINDE, F., HVID, I., Clin Biomech., **13**, 1998, p. 351.
7.GUPTA, A., BHAT, S., JAGDALE, P. R., CHAUDHARI, B. P., LIDGREN, L., GUPTA, K. C., & KUMAR, A., Tissue Engineering. Part A, **20**, nr. 23-24, 2014, p. 3101.
8.KOCK, N.B., SMOLDERS, J. M., VAN SUSANTE, J. L., BUMA, P., VAN KAMPEN, A., VERDONSCHOT, N. Knee Surg Sports Traumatol Arthrosc., **16**, 2008, p. 461.
9.HANGODY, L., KISH, G., KARPATI, Z., UDVARHELYI, I., SZIGETI, I., BELY, M., Orthopedics., **21**, nr. 7, 1998, p. 751.
10.BOWLAND, P., INGHAM, E., JENNINGS, L., FISHER, J., Proc IMechE Part H: J Engineering in Medicine., **229**, nr. 12, 2015, p. 879.
11.DELCOGLIANO, M., MENGHI, A., PLACELLA, G., SPEZIALI, A., CERULLI, G., CARIMATI, G., PASQUALOTTO, S., BERRUTO, M., Joints., **2**, nr. 3, 2014, p. 102.
12.BRITTBERG, M., PETERSON, L., ICRS Newsletter., **1**, 1998, p. 5. www.cartilage.org.
13.MAINIL-VARLET, P., AIGNER, T., BRITTBERG, M., et al., J. Bone Joint Surg. Am., **85** A (Suppl. 2), 2003, p. 45.
14.TRAMBITAS, C., POP, T. S., TRAMBITAS MIRON, A. D., DOROBANTU, D. C., BRINZANIUC, K., Rev. Chim. (Bucharest), **68**, no.2, 2017, p. 387.
15.ZHAO, M., CHEN, Z., LIU, K., WAN, Y., LI, X., Luo, X., et al., Journal of Zhejiang University. Science. B, **16**, nr. 11, 2015, p. 914.
16.BUMA, P., PIEPER, J. S., VAN TIENEN, T., VAN SUSANTE, J. L., VAN DER KRAAN, P. M., VEERKAMP, J. H., VAN DEN BERG, W. B., VETH, R. P., VAN KUPPEVELT, T. H., Biomaterials, **24**, 2003, p. 3255.

17.ENEA, D., GUERRA, D., ROGGIANI, J., CECCONI, S., MANZOTTI, S., QUAGLINO, D., PASQUALI-RONCHETTI, I., GIGANTE, A., International Journal of Immunopathology and Pharmacology, 26, 2013, p. 917.
18.ABARRATEGI, A., LOPIZ-MORALES, Y., RAMOS, V., CIVANTOS, A., LOPEZ-DURAN, L., MARCO, F., LOPEZLACOMBA, J. L., Journal of Biomedical Materials Research Part A, **95**, 2010, p. 1132.
19.BELL, A. D., LASCAU-COMAN V., SUN, J., CHEN, G., LOWERISON, M. W., HURTIG, M.B., HOEMANN, C. D., Cartilage, **4**, 2013, p. 131.
20.GUZMAN-MORALES, J., LAFANTAISIE-FAVREAU, C. H., CHEN, G., HOEMANN, C. D., Osteoarthritis Cartilage, **22**, 2014, p. 323.
21.IGARASHI, T., IWASAKI, N., KAWAMURA, D., KASAHARA, Y., TSUKUDA, Y., OHZAWA, N., ITO, M., IZUMISAWA, Y., MINAMI, A., Journal of Biomedical Materials Research Part A, **100**, 2012, p. 180.
22.SUKEGAWA, A., IWASAKI, N., KASAHARA, Y., ONODERA, T., IGARASHI, T., MINAMI, A., Tissue Engineering Part A, **18,** 2012, p. 934.
23.AULIN, C., JENSEN-WAERN, M., EKMAN, S., HAGGLUND, M., ENGSTRAND, T., HILBORN, J., HEDENQVIST, P., Laboratory Animals, **47**, 2013, p. 58.
24.MARMOTTI, A., BRUZZONE, M., BONASIA, D. E., CASTOLDI, F., ROSSI, R., PIRAS, L., MAIELLO, A., REALMUTO, C., PERETTI, G. M., Knee Surgery, Sports Traumatology, Arthroscopy, **20**, 2012, p. 2590.
25.SOLCHAGA, L.A., YOO, J. U., LUNDBERG, M., DENNIS, J.E., HUIBREGTSE, B. A., GOLDBERG, V. M., CAPLAN, A. I., Journal of Orthopaedic Research, **18**, 2000, p. 773.
26.KON, E., FILARDO, G., PERDISA, F., VENIERI, G., MARCACCI, M., Journal of Experimental Orthopaedics, **1**, 2014, P. 10.
27.*** http://jri-ltd.com/product-range/orthobiologics/maioregen/
28.KON, E., FILARDO, G., BRITTBERG, M., BUSACCA, M., CONDELLO, V., et al, Knee Surg Sports Traumatol Arthrosc, 2017, DOI 10.1007/s00167-017-4707-3.
29.EFE, T., THEISEN, C., FUCHS-WINKELMANN, S., STEIN, T., GETGOOD, A., ROMINGER, M. B., PALETTA, J. R., SCHOFER, M. D., Knee Surgery, Sports Traumatology, Arthroscopy, **20,** 2012, P. 1915.
30.KON, E., DELCOGLIANO, M., FILARDO, G., FINI, M., GIAVARESI, G., FRANCIOLI, S., MARTIN, I., PRESSATO, D., ARCANGELI, E., QUARTO, R., SANDRI, M., MARCACCI, M., J Orthop Res, **28**, nr. **1**, 2010, p. 116.
31.KON, E., MUTINI, A., ARCANGELI, E., DELCOGLIANO, M., FILARDO, G., NICOLI ALDINI, N., PRESSATO, D., QUARTO, R., ZAFFAGNINI, S., MARCACCI, M., J Tissue Eng Regen Med, **4,** nr. 4, 2010, p. 300.
32.AHMED, T. A., HINCKE, M. T., Tissue Eng Part B Rev., **16**, nr.3, 2010, p. 305.
33..LITTLE, C. J., BAWOLIN, N. K., CHEN, X., Tissue Eng Part B Rev, 17, nr. 4, 2011, p. 213.
34.VIKINGSSON, L., GALLEGO FERRER, G., GOOMEZ-TEJEDOR, J. A., GOMEZ RIBELLES, J. L., Journal of the Mechanical Behavior of Biomedical Materials, 32, 2014, p. 125.
35.MARTINEZ-DIAZ, S., GARCIA-GIRALT, N., LEBOURG, M., et al, Am J Sports Med, 38, nr. 3, 2010, p. 509

Manuscript received: 15.11.2017